# DETERMINING THE CHARACTERISTICS OF ANVIL AND THUNDERSTORM LIGHTNING FOR USE IN THE LIGHTNING LAUNCH CONTROL CRITERIA AT CAPE CANAVERAL AIR FORCE STATION AND KENNEDY SPACE CENTER

Zachary N. Tamurian*[1], Henry E. Fuelberg[1], William P. Roeder[2]  
[1] Florida State University, Tallahassee, FL  
[2] 45th Weather Squadron, Patrick AFB, FL

## 1. INTRODUCTION

The 45th Weather Squadron (45WS) provides weather support to America's space program at Florida's Cape Canaveral Air Force Station (CCAFS), Kennedy Space Center (KSC), and Patrick Air Force Base (PAFB). The greatest cloud-to-ground (CG) lightning flash densities in the U.S. occur along the Florida peninsula during the warm season (May-September; Rudlosky and Fuelberg 2010). Since CCAFS/KSC lies within Florida's "Lightning Alley", summer thunderstorms and associated hazards are a special concern for space launches and all other outdoor activities at CCAFS/KSC. Therefore, the 45WS uses the Lightning Launch Commit Criteria (LLCC) to help minimize hazards from lightning (both naturally occurring and triggered) and vehicle electrification during the ascent phase of launch from CCAFS/KSC (McNamara 2009, Willett and Merceret 2010).

McNamara et al. (2010) and Merceret and Willett (2010) provide a history of the LLCC and describe its most recent revisions in 2009. Additional history, evaluation practices, and the previous 2005 LLCC are discussed by Roeder and McNamara (2006). The following descriptions are taken from these papers, except where noted. A triggered lightning strike to an Atlas/Centaur-67 rocket shortly after launch from CCAFS on 26 March 1987 led to the destruction of the launch vehicle and payload. This event led to a complete revision of the lightning rules and began the "modern" era of the LLCC. Since rocket-triggered lightning poses such a significant threat, many of the LLCC concern this topic. An important aspect of the LLCC is to avoid compromising the rocket's in-flight termination system. Space launches under USAF, NASA, and FAA governance must follow the same LLCC. Since implementation of the "modern" LLCC after the Atlas/Centaur-67 accident in 1987, no space launch using those rules has resulted in a triggered or natural lightning event.

The LLCC consist of eleven major rules that consider different aspects of the lightning threat. The criteria are complex and require specially trained meteorologists to evaluate them operationally. The LLCC underwent a major upgrade during 2005, and were most recently revised in 2009. Table 1 summarizes the current LLCC. Three of the LLCC were significantly changed in the 2009 upgrade: 1) Attached Anvil Clouds, 2) Detached Anvil Clouds, and 3) Debris Clouds. A fourth LLCC was removed (i.e., the Electric Field Aloft rule) due to the unavailability of the required observations.

The Attached Anvil Cloud LLCC was modified to allow closer and/or sooner approach to the cloud under some conditions. This was based in part on the analysis of electric fields as a function of distance from the anvil cloud (Merceret et al. 2008) and in part on further analysis of ABFM-II data (Dye et al. 2007). A new stand-off distance of 3 n mi was added, sometimes replacing 5 n mi. A new safe condition for anvil clouds also was added. Specifically, launch within various distances of anvil clouds now is allowed under some conditions if those clouds are warmer than 0°C. Modifications to the Detached Anvil Cloud LLCC are very similar to those made to the Attached Anvil LLCC. The Debris Cloud LLCC also was modified to allow closer and/or sooner approach under some conditions, based on further analysis of the ABFM-II data (Dye et al. 2007). A new stand-off distance of 3 n mi was added under some conditions. In addition, launch within 5 n mi now is allowed if the debris cloud is warmer than 0°C and the Volume Averaged Height Integrated Radar Reflectivity (VAHIRR) criteria are met. The Electric Field Aloft rule was removed from the LLCC since there is no practical way to evaluate it operationally.

**Table 1.** Quick reference for the 2009 LLCC (after McNamara et al. 2010).

| No. | Name | **Avoid** launch if . . . |
|---|---|---|
| 1 | Surface Electric Fields | ≥ 1000 V/m, ≤ 5 n mi, ≤ 15 min unless . . . . (see appendices in McNamara et al. (2010) |
| 2 | Lightning | Lightning or thunderstorm cloud producing lightning ≤ 10 n mi and ≤ 30 min unless . . . |
| 3 | Cumulus Clouds | Cloud tops ≤ -20℃ and ≤ 10 n mi<br><br>Cloud tops ≤ -10℃ and ≤ 5 n mi<br><br>Cloud tops ≤ -5℃ and ≤ 0 n mi unless . . . (see appendices in McNamara et al. (2010) |
| 4 | Attached Anvil Clouds | ≤ 10 n mi to > 5 n mi and ≤ 30 min since lightning, unless anvil within 10 n mi and ≤ 0℃<br><br>≤ 5 n mi to > 3 n mi and ≤ 3 h since lightning, unless anvil within 5 n mi and ≤ 0℃<br><br>≤ 3 n mi, unless anvil within 5 n mi, ≤ 0℃, and VAHIRR criteria met |
| 5 | Detached Anvil Clouds | ≤ 10 n mi to > 3 n mi and ≤ 30 min since lightning, unless anvil within 10 n mi and ≤ 0℃<br><br>≥ 0 n mi to ≤ 3 n mi and ≤ 30 min since lightning, unless anvil within 5 n mi, ≤ 0℃, and VAHIRR criteria met<br><br>≥ 0 n mi to ≤ 3 n mi and > 30 min to ≤ 3 h since lightning, unless field mill and radar criteria met or anvil within 5 n mi ≤ 0℃ and VAHIRR criteria met<br><br>Unless ≥ 4 h since lightning and ≥ 3 hr since detachment<br>or<br>anvil within 5 n mi ≤ 0℃ and VAHIRR criteria met |
| 6 | Debris Clouds | ≥ 0 n mi to ≤ 3 n mi, and ≤ 3 h since detach, unless radar criteria and field mill criteria met<br>or<br>debris within 5 n mi, ≤ 0℃, and VAHIRR criteria met<br><br>Unless debris ≤ 5 n mi, ≤ 0℃, and VAHIRR criteria met |
| 7 | Disturbed Weather | Flight through (see Appendix-1 and Appendix-2 for details) |
| 8 | Thick Cloud Layers | ≥ 4500 ft thick with parts ≤ 0℃ to ≥ -20℃, or connected to thick cloud layer within 5 n mi |
| 9 | Smoke Plumes | Flight through cumulus formed from smoke plume or ≤ 60 min detach |
| N/A | Electric Field Aloft | Removed |
| 10 | Triboelectrification | Flight through any cloud ≤ -10℃ and velocity ≤ 3000 ft/sec, unless treated or tested/analyzed |
| 11 | Good Sense | Notify Launch Decision Authority if risk of triggered lightning not otherwise covered is suspected |

While the 2009 LLLC provide an extremely high level of safety against natural and rocket triggered lightning to in-flight space launch vehicles, some believe that they could be relaxed to provide increase launch availability and significant cost savings while still providing excellent safety. For example, McNamara et al. (2010) listed a number of studies that should be conducted to determine if further refinements are appropriate. One of their major recommendations was radar and lightning climatologies of attached and detached anvils. These suggested topics provided the motivation for our research.

Several LLCC definitions were changed in 2009. In particular, the definition of an anvil cloud was changed to require the upper outflow, or blow-off, to come from convective clouds reaching -10℃ or colder. This prevents warmer anvil-like clouds with insufficient electrification from needlessly cancelling a launch. The VAHIRR criteria were moved to the definitions section to avoid repeating the same complex verbiage in other LLCC and to allow easier LLCC evaluation. The definitions also clarify that the anvil cloud is not considered part of the parent thunderstorm for use in calculating thunderstorm distance.

Advances in lightning detection technology over the past two decades have provided new insights into the occurrence of both intra-cloud (IC) and CG flashes within thunderstorm anvils (e.g., Patrick 2009). These studies suggest that IC and CG flashes are common in anvils and can occur at great distances from the parent convection. Patrick (2009) noted that few studies have examined the threat posed by CG flashes far removed from the greatest reflectivity, and that mapping IC flash data in real time helps forecasters visualize threat areas outside of the main convective cores.

Recent studies have clarified the occurrence of CG flashes that originate inside the convective core but strike the ground outside the main convection. Since these side flashes often strike the ground under clear skies, they commonly are referred to as "bolts from the blue". Krehbiel (2009) noted that they are relatively common in normally electrified storms and usually transfer negative charge to ground. Side flashes originate as normal IC discharges between the upper positive and main negative charge regions. However, the upper positive charge becomes depleted with respect to the main negative charge resulting in a side flash that transfers negative charge to ground (Krehbiel 2009). These findings suggest that side flashes must be considered when evaluating the lightning threat outside the region of strong convection. The present study of side

flashes provides information about how far from the horizontal anvil edge a flash can extend. This can be used to refine both LLCC and the lightning advisories used by 45WS to provide lightning safety for personnel and resource protection (Weems et al. 2001).

The anvil region often is difficult to define, and typically exhibits a complex charge distribution (Weiss 2009). The main negative and upper positive charge can propagate from the main convection into the anvil, and a negative screening layer often lies above (Weiss 2009). Thus, anvil flashes can initiate between the positive charge region (middle) and both the negative screening layer (above) and main negative charge layer (below). Weiss (2009) found that reflectivity cores within the anvil (stratiform) region were favored for both IC and CG flashes. Interestingly, they documented a CG flash in an anvil that initiated when the reflectivity maximum descended below the melting level (0°C), and suggested that a down hanging reflectivity maximum may transport charge toward the ground resulting in a CG flash. This is consistent with the 45 WS's anecdotal experience where CG flashes from anvil clouds are more likely from pockets of higher reflectivity, especially ≥ 42 dBZ (Roeder and Pinder 1998), and from volumes of reflectivity below the main anvil cloud.

The complex nature of charge and lightning in anvil clouds, and CG flashes that strike the ground outside the main convection, motivate our research. Weiss (2009) noted that the analysis of anvil lightning also can help determine the lifetime of charge in the anvil region. The lifetime of charge is important to understanding the triggered lightning threat posed by anvil and debris clouds. Patrick (2009) stated that analyzing both total lightning and radar reflectivity is needed to properly address lightning occurrence outside regions of strong convection. Therefore, our research combines these data sources to develop a lightning and radar climatology of IC and CG flashes outside of the main convective core to help improve the utility of the LLCC in operations at CCAFS/KSC.

## 2. DATA

We analyzed both IC and CG data as well as WSR-88D and model-derived data. Operations at the 45WS are aided by the Four-

Dimensional Lightning Surveillance System (4DLSS) which consists of the Cloud-to-Ground Lightning Surveillance System (CGLSS) and Lightning Detection and Ranging (LDAR) networks. Roeder (2009) described recent upgrades to the 4DLSS that significantly improve the ability of the 45WS to evaluate the lightning threat. The most important 4DLSS upgrades for the present study are the reduced radial smearing of LDAR radiation sources and detection of individual CG strokes rather than CG flashes and multiplicity (i.e., number of return strokes).

The primary purpose of CGLSS is to assess the likelihood of induced current damage to the electronics of payloads, space launch vehicles, and key facilities (Stano et al. 2010, Boyd et al. 2005). CGLSS utilizes sensors that are similar to those employed by the National Lightning Detection Network (NLDN; owned and operated by Vaisala Inc.). However, CGLSS has greater detection efficiency and location accuracy than the NLDN because its sensors are separated by smaller distances (Boyd et al. 2005). CGLSS provides 98% detection efficiency and 250 m location accuracy, if all the sensors are used in solving for lightning location (Roeder et al. 2000). CGLSS sensors are blinded by some strong nearby strokes, e.g., 28% of strokes ≥ 50 kA are missed, which is 2.8% of all strokes (Ward et al. 2008). As a result, we used NLDN data to supplement the CG data detected by the CGLSS network to account for these unreported flashes. We added a NLDN flash to the CGLSS data set only if its peak current was ≥ 50 kA and no CGLSS flash was reported within 560 m and 3 s of the NLDN flash (Ward et al. 2008). If a CGLSS flash was reported within these spatial and temporal constraints, the NLDN flash was added as done by Melvin and Fuelberg (2009).

The LDAR network at KSC detects most IC flashes and the upper portions of CG strikes with a detection efficiency greater than 90% within 100 km of the network's center (Boccippio et al. 2001). The efficiency improves to 99% when events occur within 25 km of the network's center (Maier et al. 1995; Murphy et al. 2000; Stano et al. 2010). It is important to differentiate between individual LDAR sources and flash detections. LDAR may detect only 70% of the individual sources within the network, but with typically thousands of sources per flash, the flash detection rate is close to 100%.

The Gibson Ridge Level II Analyst (GR2-Analyst) software was used to display the KMLB WSR-88D radar data and thereby select storms for possible additional analysis. The software was especially useful in locating storms having anvils. Figure 1 shows the 0 dBZ isosurface that defines the volumes (cloud edge) of two storms that were investigated further. Previous research has shown that 0 dBZ is a good proxy for cloud edge (NASA 2010).

The Warning Decision Support System – Integrated Information (WDSS-II; Lakshmanan et al. 2007) software is more sophisticated than GR2-Analyst. WDSS-II was used to simultaneously view and manipulate lightning, radar, and model-derived data. The software contains algorithms that enable the processing of the base lightning and WSR-88D data into higher-order parameters. Many 3-D radar parameters are computed by merging data from the WSR-88D in Melbourne, FL with hourly analyses from the 20 km version of the Rapid Update Cycle (RUC) mesoscale model (Lakshmanan et al. 2006). These merged radar parameters describe the 4-D reflectivity and velocity distributions and their relation to heights of various isotherm levels that are significant for thunderstorm charging. The WDSS-II cross-section tool is used to measure the flash distances.
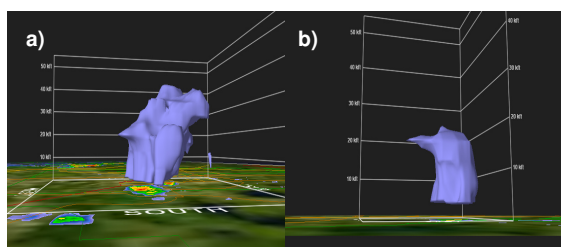


**Figure 1. a)** GR2-Analyst image displaying an anvil from the KMLB radar on 1618 UTC 8 July 2009 using an isosurface of 0 dBZ. **b)** GR2-Analyst snapshot of the 0 dBZ isosurface on 1648 UTC 8 July 2009 revealing an anvil at a lower altitude than in a).

Flash consolidation algorithms combine individual LDAR sources to reconstruct IC channels and the upper portions of CG flashes. The reduced radial smearing of LDAR source locations from the increased LDAR-II baselines (~2.5 ×) since April 2008 (Roeder et al. 2009) required the development of an enhanced flash consolidation algorithm compared to that described by Roeder (2009). The University of Oklahoma and National Severe Storms Laboratory (NSSL) have developed a flash consolidation algorithm, and recently implemented it within the WDSS-II software. This algorithm allows user-defined thresholds, error ellipses that vary with range from the LDAR center, and much faster processing time than the original KSC algorithm developed by McNamara (2002) (Melvin and Fuelberg 2009). These consolidated IC channels then can be viewed within WDSS-II and overlaid with CG flash locations as well as radar, model-derived, and satellite-based parameters. Since LDAR loses detection efficiency in the lowest 1 km of the atmosphere, the CGLSS data can be superimposed on the LDAR display to confirm that a descending flash actually became a CG strike, as is done in 45WS operations. Figures 2 and 3 illustrate the ability of the WDSS-II flash creation algorithm to lace together sources in the lower levels of the atmosphere that comprise all but the lowest part of a CG flash. WDSS-II parameters were used to make final storm selections. Both LDAR data and the WDSS-II flash creation algorithm are innovations in our study of lightning extending beyond the edge of the thunderstorm cloud and anvil.

The WDSS-II analysis environment provides many tools for processing lightning and radar data, and is an excellent platform for interrogating grids of different parameters. The WDSS-II GUI provides a Google Earth type of display that allows multiple products to be overlaid, synchronization of multiple windows, and both plan-view and cross-section analyses. Thus, WDSS-II provides an ideal environment to observe relationships between lightning and radar data sets for our thunderstorm and anvil cloud climatology. Radar parameters are used to identify the center and areal coverage of the parent convection and the location of the anvil region. The consolidated IC flashes (channels) then are used to locate the flash initiation point, flash extent (ending point), and the distance that each IC flash travels. WDSS-II permits the measurement of distance that lightning travels from the storm center and cloud edges, evaluation of radar parameters in these regions, and examination of anvil features that indicate the occurrence of IC or CG lightning.
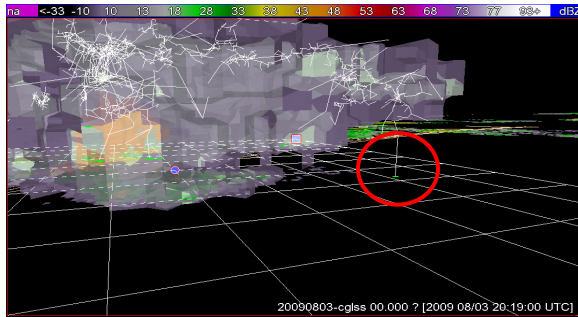
**Figure 2.** WDSS-II GUI overlay of both LDAR and CGLSS data on 2019 UTC 3 August 2009. Collocation of results from the WDSS-II flash creation algorithm and CGLSS confirms a –CG flash (red circle on the right side). The pink area on the left represents the 30 dBZ isosurface, while the nearby small red and square symbols denote the isosurface cursor.
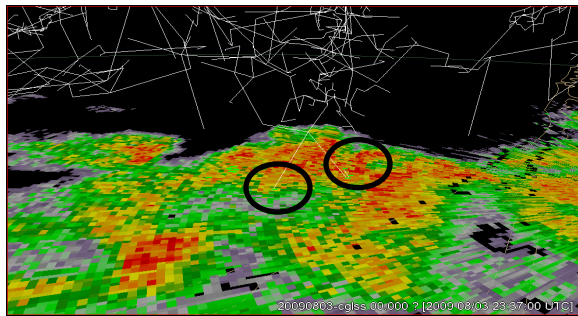


**Figure 3.** WDSS-II snapshot overlaying KMLB radar data, results from the WDSS-II flash creation algorithm using LDAR sources, and CGLSS data. Black circles (used for clarity) confirm –CG flash locations from both LDAR and CGLSS.

## 3. METHODOLOGY

The attached anvil cloud, detached anvil cloud, and lightning LLCC were the major focus of our research. Our overall goal was to develop a lightning climatology to help improve these aspects of the LLCC. We documented the spatial distribution and time evolution of total lightning and radar reflectivity in and around thunderstorms, attached anvil clouds, and detached anvil clouds near KSC to determine if some of the current LLCC thresholds are too restrictive and represent missed launch opportunities, or not restrictive enough and represent a safety risk.

The outer-cloud flash measurements were manually measured by viewing displays of LDAR and radar data. WDSS-II enables the user to rotate the display to determine the exact location where the flash exited the cloud. WDSS-II includes an isosurface tool similar to that of GR2-Analyst to approximate reflectivity

parameters based on user-defined thresholds. Flashes outside the anvil edge (0 dBZ; NASA 2010), precipitation (18 dBZ; Glickman 2000), and the convective core (30 dBZ; Kuhlman et al. 2009) were measured and recorded. This manual approach, while time consuming, was the most effective way to ensure that each flash was measured accurately. Our goal was to select only storms whose lightning flashes clearly extended outside cloud edge. This selection was the most critical and time consuming component of the research. Flashes that did not definitively fit these criteria were omitted. Automated approaches were attempted, but no currently available method accurately measured flashes outside cloud edge.

The effective range of the LDAR network determined our study domain. It was confined to within 100 km of the center of the LDAR-II network (white ring; Figure 4). This radius assured that storms would lie within the high detection efficiency regions of both CGLSS and LDAR. Due to the Earth's curvature, once a storm is greater than 100 km from the center of the LDAR network, the vertical error becomes too great to effectively use three-dimensional LDAR data. For our study, priority was given to flash events occurring within 60 km, and no event was farther than 100 km from the center of the LDAR network.

Before individual flashes could be selected for measurement, the LDAR and CGLSS data were processed by algorithms within WDSS-II. Most WDSS-II algorithms act as filters, inputting one or more parameters and writing out one or more computed parameters (Lakshmanan et al. 2007). The outputs of a WDSS-II algorithm can be used to visualize data directly, to provide information in decision making, and as input to other algorithms. Individual LDAR sources were combined into flashes using both spatial and temporal criteria in the WDSS-II software. Collocated LDAR source events were considered part of the same flash only if they were within 300 ms of each other (Lakshmanan et al. 2007). In addition, a distance formula within the WDSS-II flash creation algorithm (called w2lmaflash) consolidated simultaneous events into flashes only if the sources were within a specified distance from the center of the network (Lakshmanan et al. 2007). Besides the consolidation, the software writes to files

information about the individual flashes, flash extent densities, and flash initiation densities. Since WDSS-II processes data only from Lightning Mapping Array (LMA) networks, a program was written to format the KSC LDAR data into LMA form.
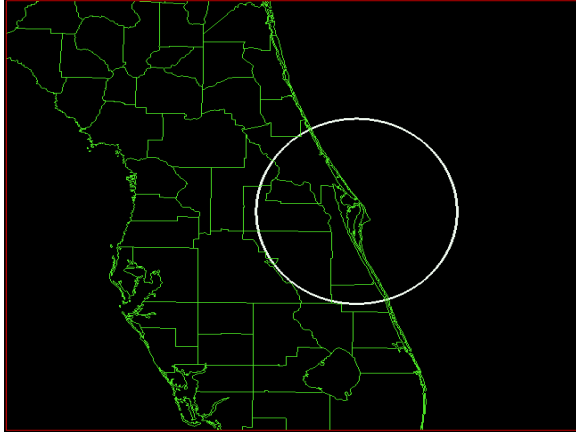


**Figure 4.** WDSS-II snapshot of the 100 km domain extending from the central location of the LDAR-II network. All measured lightning flashes (CG and IC) were within this area to ensure the accuracy of both the LDAR data and WDSS-II flash creation algorithm.

Our rigid selection criteria limited the available days to study. To ensure that our data set was robust, we first examined archived flash density data from NASA's Short-term Prediction Research and Transition Center (SPoRT) program. SPoRT provides both real-time and archived source densities from KSC's LDAR network. SPoRT's 1 × 1 km grid allowed us to view archived data from 2008-11. Based on the SPoRT data, we chose 30 days during the warm seasons (May-September) of years 2008 to 2011 when lightning densities were the greatest around KSC, especially downwind from the cores of storms. We also analyzed archived skew-T log p diagrams from Tampa to aid our search of strong wind shear environments. All 30 days showed moderately strong westerly shear. Individual storms first were located using GR2-Analyst and later analyzed using WDSS-II.

As noted earlier, we required that flash initiation points on these days be located within our domain of 100 km radius from the center of the LDAR network. Most lightning was located near the storm's core (i.e., 30 dBZ). However, a storm's LDAR sources often spread into the anvil region (i.e., 0 dBZ) in environments of moderately strong westerly shear. An anvil was defined if the farthest edge of the cirriform region extended at least 5 n mi from the edge of the 30

dBZ reflectivity after rotating the storm to obtain a side view using the WDSS-II GUI. There originally were 130 attached anvils in our data set, each consisting of at least one flash (IC or CG) that extended outside the cloud edge. However, when the anvils were tracked until they extended outside our domain, 30 anvils were rejected, leaving a final data set of 100 anvils. The majority of the 100 attached anvils later became detached. From this group, 20 detached anvils produced only a single flash outside cloud edge. The remaining 80 detached anvils produced no flashes outside cloud edge. Table 2 describes our final data set.

**Table 2.** The number of flashes and days that comprise our data set.

| Category | Flash count | Number of flash days |
|---|---|---|
| IC lightning outside thunderstorm cloud edge (0 dBZ) | 1175 | 30 |
| IC lightning outside attached anvil (0 dBZ) | 200 | 14 |
| IC lightning outside detached anvil (0 dBZ) | 20 | 6 |
| IC lightning outside core (30 dBZ), inside anvil edge (0 dBZ) | 895 | 30 |
| CG lightning along attached anvil motion (i.e., ≥ 0 dBZ) | 115 | 16 |
| CG lightning outside attached anvil (0 dBZ) | 5 | 2 |
| CG lightning outside precip. and cloud edge (18; 0 dBZ) | 80 | 22 |

The specific topics that we investigated are described below along with WDSS-II-derived graphic examples of our methodology for each.

Our first task was to measure the distance that IC flashes extended outside of the thunderstorm cloud edge (i.e., 0 dBZ) and to calculate distributions of these distances. An example of an IC flash measurement using WDSS-II is illustrated in Figure 5 using the cross-section tool. The cross-section display (right) integrates both a vertical slice (top-left; Kft) and a constant altitude plan position indicator (CAPPI [n mi]; bottom-left). We obtained the best view of each flash outside the cloud edge by appropriately rotating the WDSS-II display.
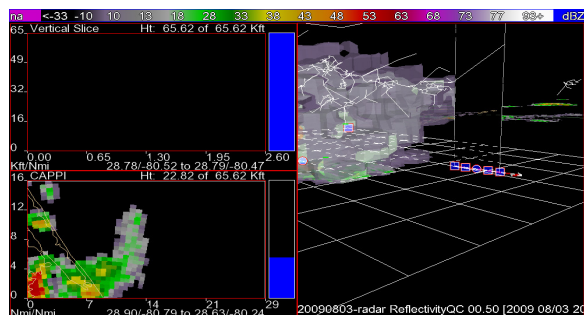
**Figure 5.** WDSS-II display of a thunderstorm flash (IC) outside of the cloud edge using both the cross-section tool and isosurface box to determine the extent of the cloud (0 dBZ; purple) and precipitation (18 dBZ; white). The LDAR flash creation algorithm laces together individual LDAR sources both spatially and temporally to define a flash. Note the distance measurement tool in the right panel (n mi). The upper left panel shows no echoes since the measurement was made outside cloud edge.

We next focused on anvils that formed within 100 km of KSC. Our task was to measure the distance that IC lightning traveled outside the edge of the attached anvil (0 dBZ), using the same methodology (Figure 6) of the previous task (Figure 5).
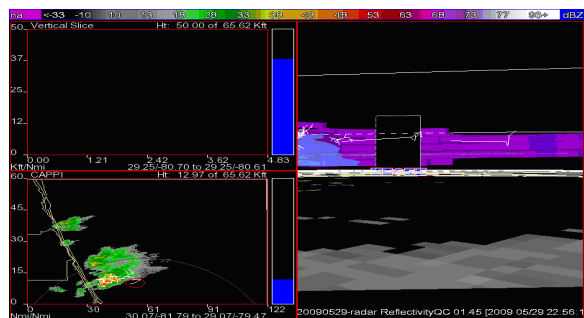


**Figure 6.** WDSS-II snapshot of a lightning flash (IC) outside the edge (0 dBZ; purple) of an attached anvil and downwind of the convective core (30 dBZ; blue). The flash (red circle; bottom left) extends 4.83 n mi from the edge of the attached anvil.

Lightning in anvils sometimes persists after detachment. Our next task was to create a distance frequency distribution for IC lightning extending perpendicular and outside the edge of the detached anvil (0 dBZ). Figure 7 reveals a flash that clearly exits the detached anvil edge.

Our next assignment was to measure the total lightning (IC and CG) inside the attached anvil (0 dBZ; Figure 7). The previous task investigated IC flashes beyond the anvil edge.
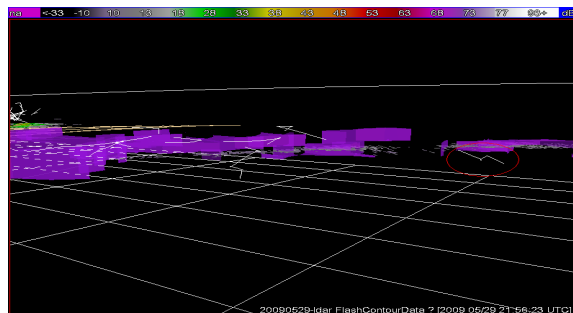


**Figure 7.** WDSS-II snapshot of a flash (red oval) extending outside the edge of a detached anvil edge (0 dBZ; purple). The anvil extends 40 n mi offshore of KSC. The flash extends ≤ 10 n mi from cloud edge. No previous detached anvil flashes were detected outside the cloud edge.
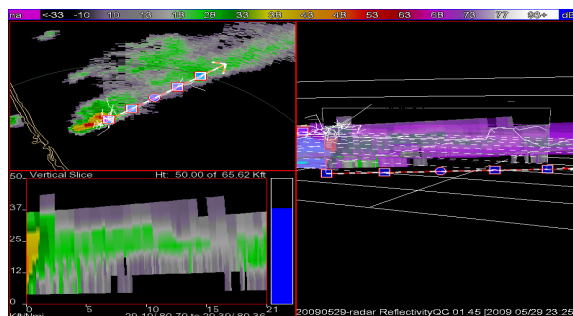


**Figure 8.** IC flash extending ≥ 20 n mi inside the attached anvil region (≥ 0 dBZ; purple) using the cross-section measuring tool and an isosurface box. The isosurface box outlines the approximate threshold of the anvil's edge (0 dBZ).

We then considered anvil lightning initiated from the core of the storm. We defined the reflectivity threshold of the core to be 30 dBZ using the WDSS-II software's isosurface tool and then measured the farthest extent of the initial flash from the edge of the 30 dBZ echo (e.g., Figure 9). We created both a frequency and distance distribution of the first anvil flash.

The final task was to investigate CG flashes extending beyond the thunderstorm cloud edge (0 dBZ; i.e., "bolts from the blue") and its precipitation edge (18 dBZ). We accomplished this task using the combination of LDAR and CGLSS data. Figure 10 shows a – CG flash outside cloud edge. The WDSS-II flash creation algorithm laces the LDAR sources into a flash collocated with the CGLSS data. We created a distance distribution of CG lightning outside of thunderstorm precipitation and outside of thunderstorm cloud edge.
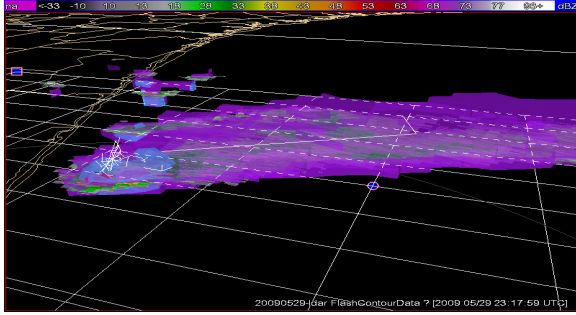
**Figure 9.** First anvil flash (IC) extending from the thunderstorm convective core (30 dBZ; blue) into the anvil region (≥ 0 dBZ; purple). The anvil formed offshore of KSC on 29 May 2009 and stretched ≥ 10 n mi from the storm core.
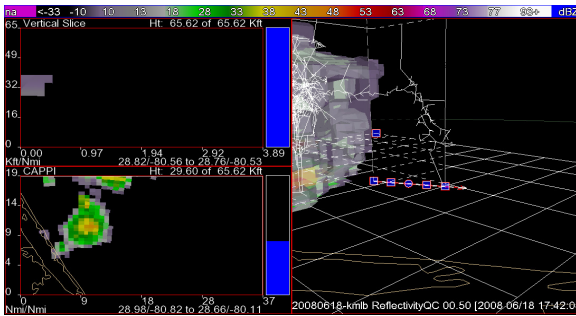


**Figure 10.** –CG flash "bolt from the blue" outside the cloud edge of the thunderstorm (0 dBZ; purple). The flash extended 3.89 n mi from the thunderstorm cloud edge on 1742 UTC 18 June 2008. CG flashes outside the precipitation core (18 dBZ; gray) can extend ≥ 10 n mi.

## 4. RESULTS

The science and the operational utility of this study are significantly improved by a best-fit general extreme value distribution and its integration to determine the probability of > X to infinity, where X is any desired distance. Extreme value theory is a separate branch of statistics that deals with outlier events. These data are extreme in the sense of being unusually large, and by definition are also rare (Wilks 2006). Extreme-value statistics often are of interest because the physical processes generating extreme events, and the societal impacts that occur because of them, also are large and unusual. For example, the probability of lightning extending > 10 n mi gives an indication of the safety provided by the Lightning Rule in the LLCC. We can specify a desired level of safety to calculate the distance from cloud edge that provides that safety. The probability density function (PDF) given by equation (1) below describes the relative likelihood that a random event will occur. The total frequency of all classes less than the upper

class boundary of a given class is called the cumulative distribution function (CDF).

$$f(x) = 1/\sigma \; \exp(1-(1+kz)^{-1/k})(1+kz)^{-1-1/k} \quad \textbf{(1)}$$

$$z = (x-\mu)/\sigma \quad \textbf{(2)}$$

To our knowledge this is the first statistical study of lightning flashes measured from the edges of clouds. Thus, our results cannot be compared with those of others. Figure 11 is a distance frequency distribution of the 1175 IC flashes that extended outside the edge of thunderstorm clouds (0 dBZ). The majority (~98%) extend ≤ 10 n mi with a mean distance of 3.89 n mi. The percentage of IC flashes extending ≥ 10 n mi is 1.71%. A small percentage of flashes (~1%) extends ≥ 15 n mi beyond the cloud edge. A cumulative IC flash probability distribution (Figure 12) shows an increase in percentage for flashes extending ≥ 5 n mi from the thunderstorm cloud edge. Outer-cloud IC flashes ≤ 5 n mi occur 65% of the time. The small percentage exceeding 10 n mi is especially important for thunderstorms approaching KSC since that is the stand-off distance in the Lightning Rule of the LLCC. While the percentages of flashes (≥ 10 n mi) are small, they do represent a safety risk.
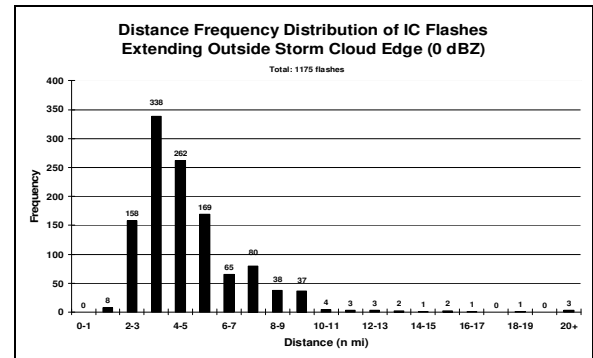


**Figure 11.** Distance frequency distribution of the 1175 IC flashes extending outside the storm cloud edge (0 dBZ).
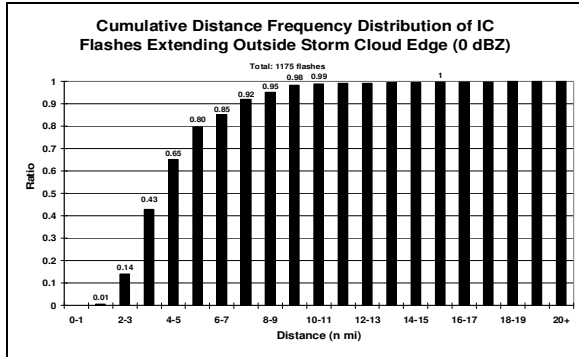
**Figure 12.** Cumulative probability distribution of 1175 IC flashes that extend beyond the thunderstorm cloud edge (0 dBZ).



**Figure 14.** Cumulative distribution function of IC flashes extending outside storm cloud edge (0 dBZ) based on extreme value theory.

The current LLCC provide a level of safety for lightning at a distance of ≤ 10 n mi. However, based on our results, the CFD (10 n mi) yields a value of 96.93% using equation (1) with the appropriate parameters (k, σ, µ; Figure 14). This percentage indicates the probability of an IC flash extending less than or equal to 10 n mi from the storm cloud edge (0 dBZ). 3.07% of IC flashes from the storm cloud extend greater than or equal to 10 n mi. The PDF (10 n mi) is 1.36%; indicating a small probability of a IC flash extending exactly 10 n mi from the storm core (0 dBZ; Figure 13).

**Table 3.** Probability (%) of IC flashes extending outside storm cloud edge (0 dBZ) at a distance (n mi) equal or less than the value listed. Values are based on extreme value theory.

| Distance (n mi) | Cum. prob. of flash ≤ distance (%) |
|---|---|
| 3 | 16.37 |
| 5 | 63.97 |
| 7 | 87.17 |
| 9 | 95.17 |
| **10** | **96.93** |
| 12 | 98.67 |
| 15 | 99.56 |



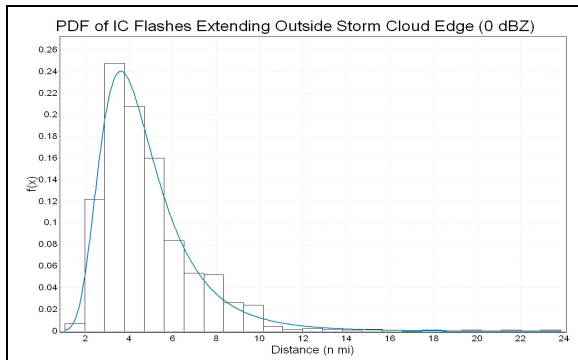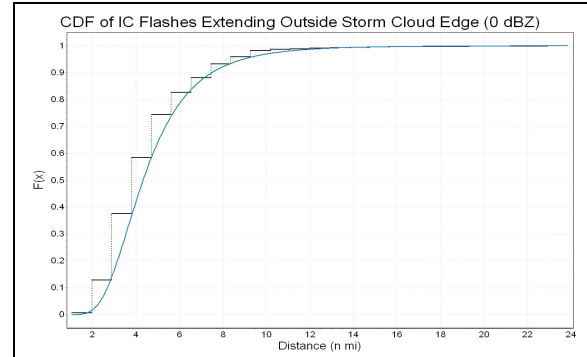**Figure 13.** Probability density function of IC flashes extending outside storm cloud edge (0 dBZ) based on extreme value theory.

Electrified anvil clouds over KSC can emanate from thunderstorms that may extend as far as 200 km away if there is moderately strong westerly shear (Short et al. 2004). Mature and even detached anvils can remain electrically charged for several hours, thus posing a threat for triggered lightning if approached or penetrated by a launch or landing vehicle (Garner et al. 1997; Short et al. 2004). Short et al. (2004) studied the life cycles of 163 anvils over the Florida peninsula and coastal waters on 49 days during May-July 2001. The propagation of anvil clouds was highly correlated with the speed and direction of upper-tropospheric winds between 300-150 mb (~9-14 km altitude). Lightning activity associated with strong westerly vertical wind shear has been correlated to severe weather and anvil development in Florida (Hagemeyer and Schmocker 1991). Easterly shear can produce an anvil over KSC from convective systems over the Atlantic Ocean (Short et al. 2004).

Most lightning occurs in the core region (i.e., within the 30 dBZ region); however, dissipating storms in environments of moderately strong upper level wind shear can transfer charge to the attached anvil cloud region. Charge separation from the convective core may stimulate a spontaneous flash in the anvil. We measured (Figure 15) the distance that the first anvil flash (typically IC) traveled from the cores of each of the 100 anvils in our data set. A large percentage (~48%) of initial anvil flashes is within 3-6 n mi of the storm core. However, Figure 16 reveals that some flashes (~8%) propagate more than 10 n mi from the edge of the core.

**Distance Frequency Distribution First Attached Anvil Flash (IC) Extending From Storm Core (30 dBZ)**
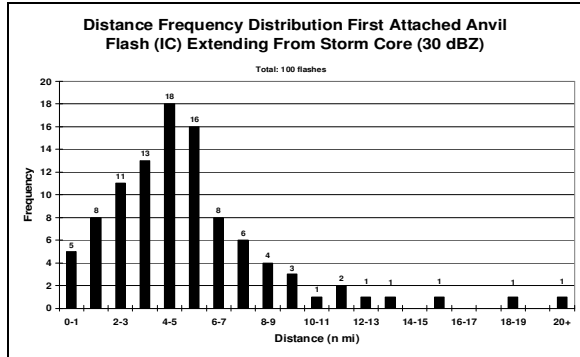
Total: 100 flashes

**Figure 15.** Distance distribution of the first anvil flash (IC) from the thunderstorm core (30 dBZ). The total number of flashes is 100.

Based on our results, the CFD (10 n mi) yields a value of 90.65% using equation (1) with the appropriate parameters (k, σ, μ). This percentage indicates the probability of an attached anvil IC flash extending less than or equal to 10 n mi from the storm core (30 dBZ; Figure 18). A 99% level of safety is achieved at a distance ≥ 18 n mi from the storm core (30 dBZ). The PDF (10 n mi) is 2.89% (Figure 17), illustrating the distance probability of the first IC flash from the storm core (30 dBZ) extending 10 n mi. Table 4 lists flash distances with their appropriate cumulative probability percentage.
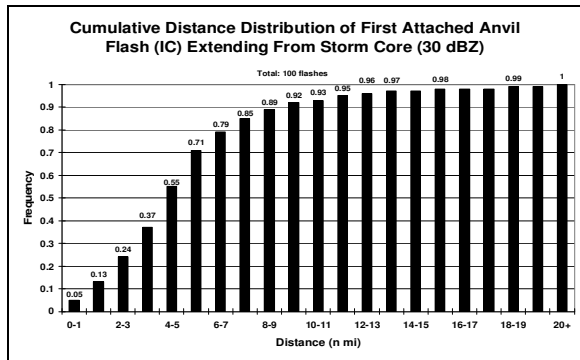
**Cumulative Distance Distribution of First Attached Anvil Flash (IC) Extending From Storm Core (30 dBZ)**

Total: 100 flashes

**Figure 16.** Cumulative probability distribution of the first anvil flash (IC; 100 flashes) from the thunderstorm core (30 dBZ).

PDF of First Attached Anvil IC Flash From Storm Core (30 dBZ)
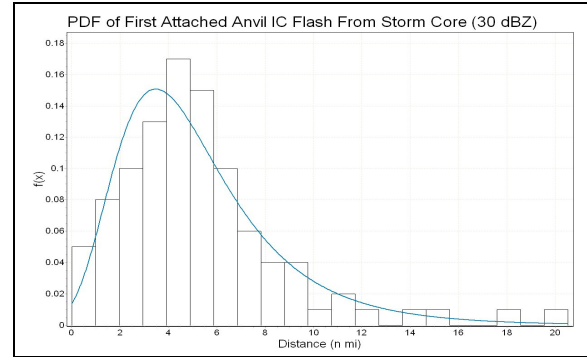
**Figure 17.** Probability density function of the first attached anvil IC flash extending from the storm core (30 dBZ) based on extreme value theory.

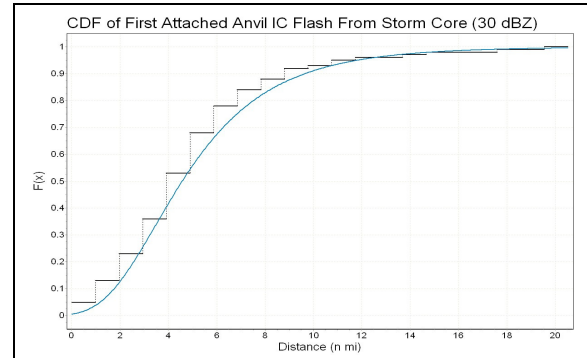CDF of First Attached Anvil IC Flash From Storm Core (30 dBZ)

**Figure 18.** Cumulative distribution function of the first attached anvil IC flash extending from the storm core (30 dBZ) based on extreme value theory.

Charging mechanisms in the anvil are complex (Short et al. 2004). The typical charge structure of an anvil cloud (Figure 19) consists of a positively charged center surrounded by a negatively charged exterior-screening layer near the top and bottom of the anvil (Marshall et al. 1989). The non-inductive charge mechanism occurs when ice crystals and graupel collide in the presence of supercooled water in the mixed phase region of the storm (Marshall et al. 1989; Short et al. 2004). An updraft can carry the lighter, positively charged particles aloft and into the anvil region. Conversely, the heavier particles (negative charge) sink to the bottom of the storm. Anvil lightning typically is IC, with the exception of spontaneous CG flashes (typically positive) in the stratiform region. In addition, there is some evidence for new charging in the anvil cloud (Dye et al. 2007), as compared to charge generated in the thunderstorm core and advected into the anvil cloud or deposited there by lightning flashes.

We measured the propagation distance of 895 IC flashes that initiated inside the core (30 dBZ) and remained inside the attached anvil

(Figure 20). Of the 895 IC flashes, 105 (~12%) extend ≥ 10 n mi from the convective core and 9 (~1%) extend ≥ 25 n mi. Table 5 illustrates the CFD for all IC flashes within the attached anvil region. It should be noted that the LLCC standoff distance of 10 n mi yields a probability of ~88% using the CFD with the appropriate parameters (Figure 22). The 99th percentile distance range is achieved at 24 n mi from the core of the storm (30 dBZ) threshold.

Lightning outside the attached anvil cloud is rather infrequent. Out of our data set of 100 attached anvils, 200 flashes extended outside the attached edge (Figure 23). The majority of flashes (~37%) were between 0 and 1 n mi outside of the 0 dBZ reflectivity threshold. 1.5% of the flashes extended ≥ 10 n mi. Table 6 is similar to Tables (3-5), but denotes the percentage of IC flashes extending outside the attached anvil edge (0 dBZ) at specified distances using the CFD. The 10 n mi standoff distance of the LLCC yields a 98.71% using the CDF. A negative exponential distribution of IC flashes extending outside the attached anvil edge (0 dBZ) is illustrated in Figure 24. Figure 25 shows the PDF with the parameters listed at the top right. Note that inserting the parameters into equation (1) yields the appropriate value of f(x) or PDF(x) at a distance 'x' from cloud edge (0 dBZ). Figure 26 is similar to 25 in which each distance's probability is cumulative to infinity. Note that the negative exponential distribution provides the best fit for IC flashes extending outside the attached anvil edge (0 dBZ).

Although most anvil flashes begin in the main convective core (≥ 30 dBZ) and propagate into the anvil, previous studies (e.g., Marshall et al. 1989; Kuhlman et al. 2009) have shown that some flashes initiate in the anvil or detached anvil. Kuhlman et al. (2009) reported anvil initiated flashes in two merging supercell storms in the Midwest. They hypothesized that the likely cause of flash initiation in the anvil was an increase in the electric field due to the convergence of anvils that brought together opposite polarities of charge at the same altitude. The flash rates at times exceeded 5 min⁻¹ until the charge was sufficiently reduced and could not be replenished by charge transport across the region of anvil lightning activity. Additional research would be needed to determine if and how often that mechanism occurs in central Florida.

We also searched for IC flashes that initiated in detached anvils. Charged regions in the anvil are short-lived, especially after detachment. Therefore, this task was the most difficult of our study. Of the 100 anvils, 80 later became detached. Twenty of the 80 detached anvils produced one IC flash that extended outside its outer edge. No detached anvil produced more than one flash that extended outside the cloud edge. Over half of these flashes extended less than 1 n mi (Figure 27). The remaining 60 detached anvils produced no flashes that extended outside the anvil. We found three IC events that extended relatively far from the detached anvil, 6.13, 3.04, and 2.76 n mi. No IC flashes extended ≥ 10 n mi outside the 0 dBZ reflectivity threshold. Since we found only one flash per storm, we could not construct a time distribution. Ultimately, we found that the first/only IC flash in the detached anvil cloud occurred within 5 min of detachment. This is most likely a result of a cutoff of charge transferred from the main core to the anvil.
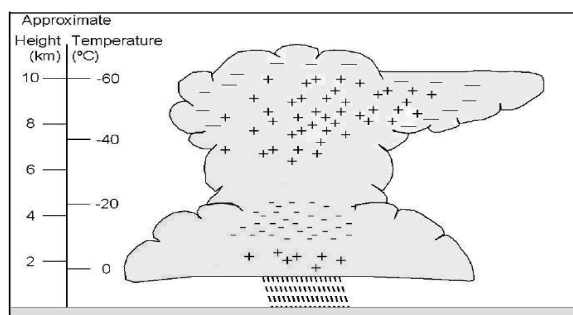


**Figure 19.** Typical structure of an anvil cloud with a positively charged center surrounded by a negatively charged exterior-screening layer near the top and bottom (after Marshall et al. 1989).
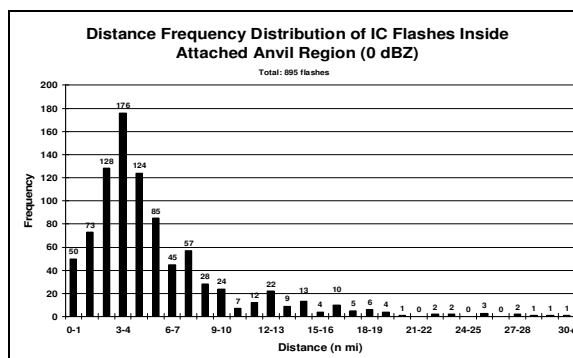


**Figure 20.** Distance frequency distribution of IC lightning inside the anvil (0 dBZ) of 895 flashes.

**Table 5.** Probability (%) of an IC flash inside the anvil region measured from the storm core (30 dBZ) based on extreme value theory.

| Distance (n mi) | Cum. prob. of flash ≤ distance (%) |
|---|---|
| 3 | 31.01 |
| 5 | 58.73 |
| 7 | 75.98 |
| 9 | 85.61 |
| **10** | **88.46** |
| 12 | 92.78 |
| 15 | 96.05 |
| 18 | 97.67 |
| 21 | 98.55 |
| 25 | 99.17 |
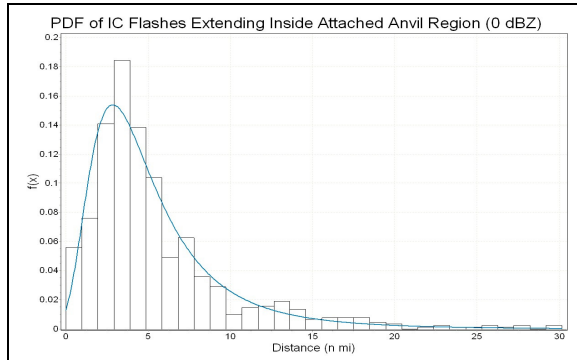


**Figure 21.** Probability Density Function of IC flashes extending inside the attached anvil region (0 dBZ) based on extreme value theory.
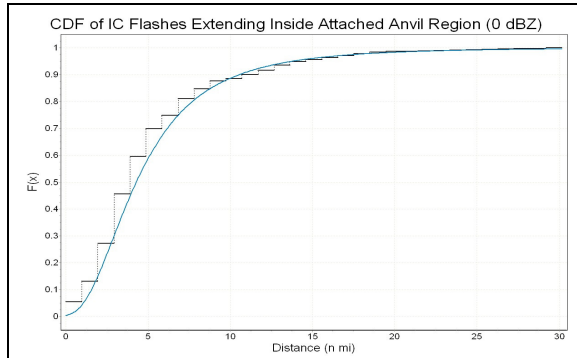


**Figure 22.** Cumulative distribution function of IC flashes extending inside the attached anvil region (0 dBZ) based on extreme value theory.
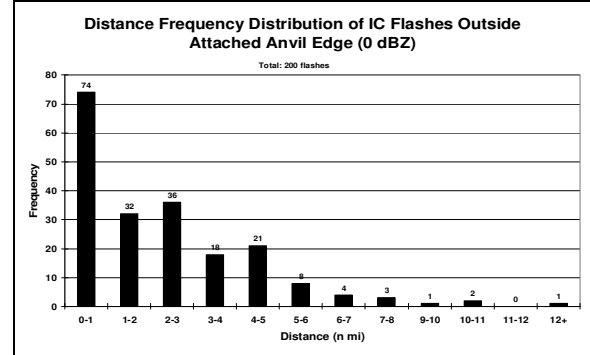


**Figure 23.** Distance frequency distribution of 200 IC flashes extending perpendicular and outside the edge of the attached anvil (0 dBZ).
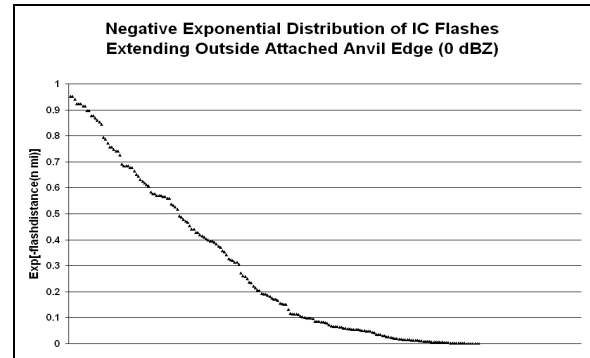


**Figure 24.** Negative exponential distribution of IC flashes that extend outside of the attached anvil edge (0 dBZ).

**Table 6.** Probability (%) of IC flashes extending outside the attached anvil cloud edge (0 dBZ) based on extreme value theory.

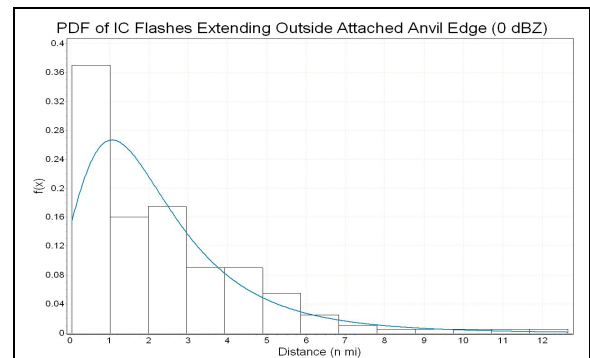| Distance (n mi) | Cum. prob. of flash ≤ distance (%) |
|---|---|
| 3 | 73.76 |
| 5 | 93.69 |
| 7 | 95.91 |
| 9 | 98.15 |
| **10** | **98.71** |
| 12 | 99.33 |



**Figure 25.** Probability density function and histogram of IC flashes extending outside the edge of an attached anvil (0 dBZ) based on extreme value theory.
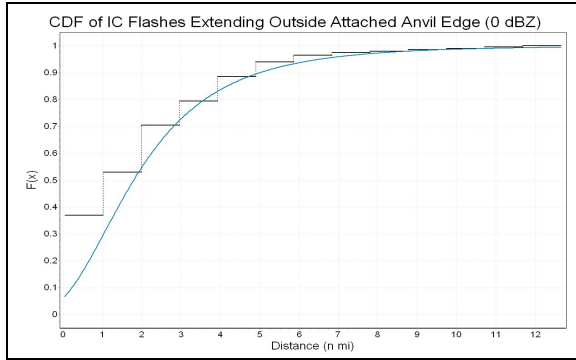
**Figure 26.** Cumulative density function and histogram of IC flashes extending outside attached anvil edge (0 dBZ) based on extreme value theory.
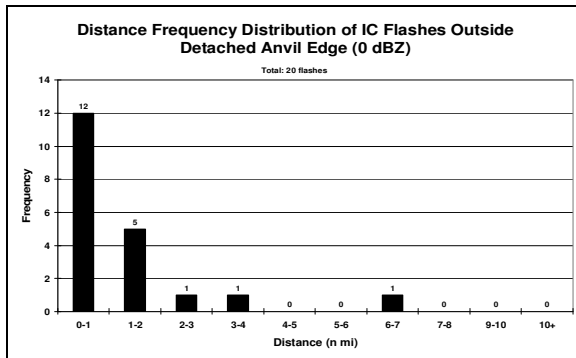


**Figure 27.** Distance frequency distribution of the 20 IC flashes that initiated in a detached anvil and extended perpendicular and outside the edge of the detached anvil (0 dBZ).

Now that the IC flashes have been described, we next consider CG flashes that remain under or extend laterally away the attached anvil region. It is not surprising that an already initiated anvil flash can extend to the ground, because anvils can contain substantial electric charge (Kuhlman et al. 2009). Electric fields and charge typically decrease with distance into the anvil because of diffusion and the electric conductivity of air (Dye et al. 2007). We located 120 CG flashes that were either under or outside the edge of attached anvils (Figure 28). Their distances vary greatly, both from the convective core and anvil edge (~52% flashes ≤ 10 n mi;  10% flashes ≥ 15 n mi).

Bolts from the blue can originate in the core of a storm or in its anvil. From our data set of 120 CG flashes, we found five that originated in an anvil, extended ≤ 3 n mi outside anvil edge, and occurred ≤ 5 min before detachment (not shown). The remaining (115) flashes propagated from the core (30 dBZ) and into the attached anvil cloud but did not extend beyond cloud edge. All detached anvils with a prior CG

flash outside anvil edge before detachment produced a single flash outside its edge within 5 min of detachment. Kuhlman et al. (2009) found that the flash repetition time exceeded the time it took for the charge to transport across the region of the anvil. However, in our five cases, the detached anvils only contained enough charge to initiate a single flash.
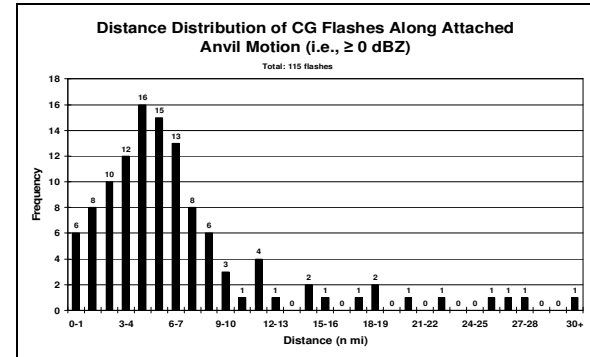


**Figure 28.** Distance frequency distribution of CG flashes along the attached anvil motion. 115 CG flashes were along the anvil motion, and five were outside the edge of the anvil.

Figure 29 illustrates a histogram and a probability density function for CG flashes inside the attached anvil motion (0 dBZ). Figure 30 represents the cumulative density function for the same criteria. Note that ~99% cumulative probability is achieved for a CG flash distance of 30 n mi across the anvil motion. A large percentage of attached anvils in our study extended over 45 n mi from the storm core (30 dBZ), and the subsequent CG flashes extended inside the attached anvil region (0 dBZ or greater).

**Table 7.** Probability (%) of CG flashes extending along the attached anvil motion (i.e., ≥ 0 dBZ) based on extreme value theory.

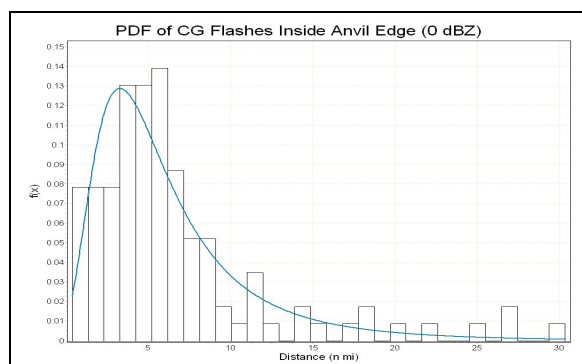| Distance (n mi) | Cum. prob. of flash ≤ distance (%) |
|---|---|
| 3 | 23.98 |
| 5 | 49.86 |
| 7 | 68.18 |
| 9 | 79.47 |
| **10** | **82.63** |
| 12 | 88.69 |
| 15 | 93.31 |
| 18 | 95.78 |
| 21 | 97.21 |
| 24 | 98.07 |
| 27 | 98.62 |
| 30 | 98.99 |

**Figure 29.** Probability density function and histogram of CG flashes extending inside anvil edge (0 dBZ) based on extreme value theory.
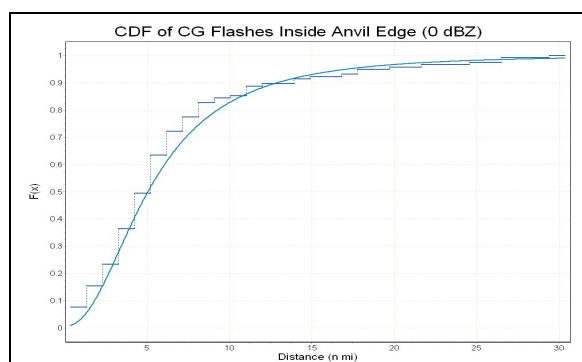


**Figure 30.** Cumulative density function and histogram of CG flashes extending inside anvil edge (0 dBZ) based on extreme value theory.
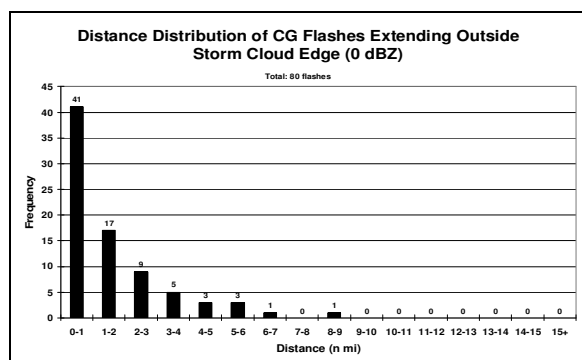


**Figure 31.** Distance distribution of the 80 CG flashes extending outside the edge of the thunderstorm cloud (0 dBZ), i.e., bolts from the blue.

We next consider bolts from the blue that do not originate in the anvil, but originate in the core of the storm. These cases should not be confused with CG flashes that extend from the core to the anvil region because these bolts strike the ground in areas with a reflectivity less than 0 dBZ. The screening layer produces a charge imbalance that enables intracloud discharges to escape outward from the storm and produce a bolt from the blue (Krehbiel 2009). We measured 80 CG (three of which

were +CG) flashes that extended either outside the edge of the thunderstorm cloud (0 dBZ) or outside the precipitation (18 dBZ; Figures 31, 32; respectively). Two CG flashes extended ≥ 10 n mi from the precipitation (11.14 and 13.03 n mi; 2.5%) and both were positive polarity. Over half of the CG flashes extended ≤ 1 n mi and none extended ≥ 10 n mi beyond the edge of the cloud (0 dBZ). A mean distance of 2.83 n mi was calculated between the precipitation threshold (18 dBZ) and the cloud edge (0 dBZ).

Three of our bolts from the blue exhibited positive polarity, and all three came from the same storm on 29 May 2009. One of the +CG flashes propagated 8.91 n mi (1643 UTC). Maximum reflectivity exceeded 55 dBZ, and propagation was westerly toward KSC. CG (IC) flash rates were ~5 (12) flashes $min^{-1}$. All flashes ceased when the storm approached the coast at 2013 UTC and quickly dissipated by 2200 UTC.
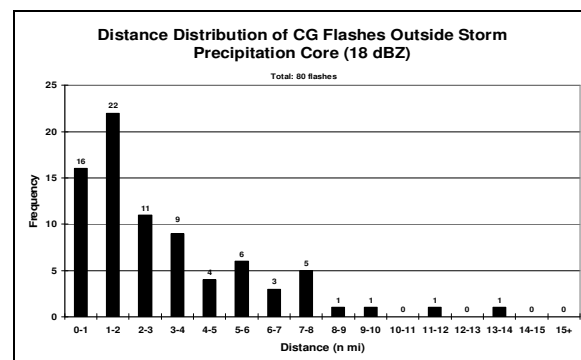


**Figure 32.** Distance distribution of the 80 CG flashes extending outside the thunderstorm precipitation threshold (18 dBZ).

Figures 33 and 34 represent probability and cumulative density functions for CG flashes extending outside the storm precipitation core (18 dBZ). The CDF (10 n mi) yields an accumulated 96.96% probability. A 99% cumulative probability is achieved at a distance of ~15 n mi from the edge of the precipitation threshold (18 dBZ). Table 8 lists the CG flash distances from the storm precipitation core (18 dBZ) with the appropriate cumulative probability of each flash at that distance.

**Table 8.** Probability (%) of CG flashes extending outside the storm precipitation threshold (18 dBZ) based on extreme value theory.

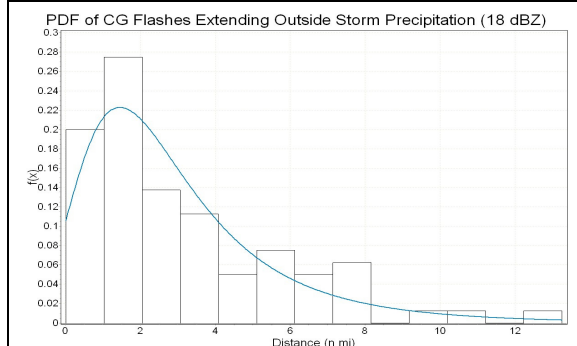| Distance (n mi) | Cum. prob. of flash ≤ distance (%) |
|---|---|
| 3 | 60.75 |
| 5 | 82.42 |
| 7 | 91.74 |
| 9 | 95.83 |
| **10** | **96.96** |
| 12 | 98.31 |
| 15 | 99.22 |



**Figure 33.** Probability density function and histogram of CG flashes extending outside storm precipitation (18 dBZ) based on extreme value theory.



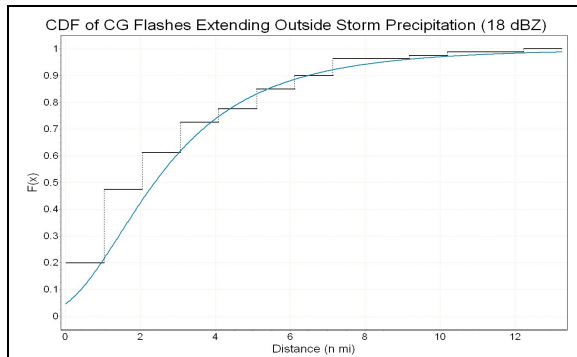**Figure 34.** Cumulative density function and histogram of CG flashes extending outside storm precipitation (18 dBZ) based on extreme value theory.

## 5. CONCLUSIONS

The 45WS provides weather support to CCAFS and KSC for launches and outdoor activities. An important part of their launch support is to evaluate and forecast the LLCC. The LLCC have been revised and upgraded to relax some criteria without sacrificing safety. McNamara et al. (2010) listed several studies that should be conducted to determine if further refinements are appropriate. One of their major recommendations was to prepare lightning "climatologies" for flashes within attached and detached anvils.

This study has documented the spatial distributions and time evolution of total lightning and radar reflectivity in and around thunderstorms, attached anvil clouds, and detached anvil clouds near CCAFS/KSC on 30 active lightning days between 2008-2011. Our goal was to determine if some of the current LLCC thresholds are too restrictive and represent missed launch opportunities, or not restrictive enough and represent a safety risk.

The WDSS-II software allowed us to ingest several data sources and to classify storm parameters for flash measurement. We analyzed 1175 IC flashes and found that 1.71% extended ≥ 10 n mi outside cloud edge (0 dBZ). In the case of CG flashes, only a small percentage (~2 %) propagated ≥ 10 n mi from precipitation.

CG flashes originating inside the convective core or its anvil can strike the ground away from the cloud edge. These bolts from the blue are common in electrified storms and typically transfer negative charge to the ground (Krehbiel 2009). Our results indicate that the vast majority of CG flashes (~94%) strike the ground ≤ 5 n mi from cloud edge (0 dBZ; Figure 35), whereas 73% of CG flashes are ≤ 3 n mi outside 0 dBZ. No bolt from the blue extended ≥ 10 n mi from cloud edge. Three positive bolts from the blue were documented, and all came from the same storm on 29 May 2009. One of the positive flashes propagated 8.91 n mi from cloud edge. The maximum reflectivity of this storm exceeded 55 dBZ, and propagation was westerly toward KSC. CG (IC) flash rates were large (~5 (12) flashes min$^{-1}$).

Charge transfer to the anvil region near KSC occurs in environments of strong westerly shear in the upper levels (~300-150 mb; Short et al. 2004). This charge sometimes remains for several hours (Kuhlman et al. 2009). The anvil region often is difficult to define and typically exhibits a complex charge distribution (Weiss 2009). Anvil initiated lightning can distribute charge after detachment, but only for a short period. We analyzed 100 anvils within 100 km of KSC; 895 IC flashes in the anvil were initiated in the core of the storms. The first core initiated flash of each anvil typically propagated ≤ 10 n mi, with the exception of a small percentage (~8%), Figure 16). 200 IC flashes extended outside the edge of the attached anvil, and 20 extended outside of detached anvils. Each

detached anvil triggered only one flash. From our data set of 120 CG flashes, we found five to be outside the anvil edge, ≤ 3 n mi, and occurring ≤ 5 min before detachment. In addition, all detached anvils with a prior CG flash outside anvil edge before detachment produced a single flash outside its edge within 5 min of its detachment.
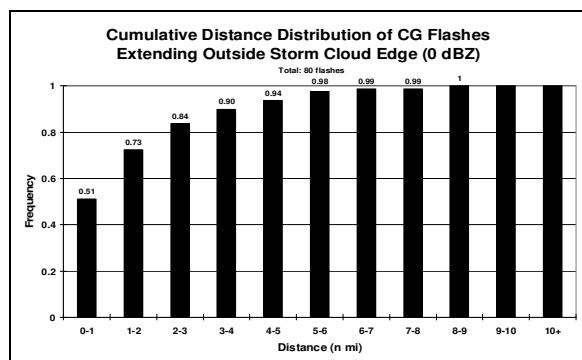
**Cumulative Distance Distribution of CG Flashes Extending Outside Storm Cloud Edge (0 dBZ)**

Total: 80 flashes

**Figure 35.** Cumulative probability distribution of 80 CG flashes extending outside the edge of the thunderstorm cloud (0 dBZ).

The threat of natural and triggered lightning has a significant impact on space launches at CCAFS/KSC (Roeder and McNamara 2006). Cellular thunderstorms produce the greatest percentage of total lightning (~84%) in our dataset, but average flash distances from the core are greatest in attached anvils (~4.98 n mi). The probability of any type of lightning extending >10 n mi from the cloud edge of a thunderstorm cell is (2.14%); from edge of anvil (0.89%). These are the two critical results from the Lightning LCC perspective.

To our knowledge this is the first study to quantify the distances that lightning can extend beyond the edge of clouds. We believe the results of this research should be considered before making additional changes to the LLCC.

## 6. REFERENCES

Boccippio, D. J., S. J. Heckman, and S. J. Goodman, 2001: A diagnostic analysis of the Kennedy Space Center LDAR network: 1. Data characteristics, *J. Geophys. Res.*, **106**, 4769–4786, doi: 10.1029/2000JD900687.

Boyd, B. F., W. P. Roeder, D. L. Hajek, and M. B. Wilson, 2005: Installation, upgrade, and use of a short baseline cloud-to-ground lightning surveillance system in support of space launch operations, *Conf. on Meteorological Applications of Lightning Data, Amer. Meteor. Soc.*, San Diego, CA.

Glickman, T.S., 2000: *Glossary of Meteorology*, 2nd Edition, American Meteorology Society, Boston, MA, 638 pp.

Dye, J. E., M. G. Bateman, H. J. Christian, E. Defer, C. A. Grainger, W. D. Hall, E. P. Krider, S. A. Lewis, D. M. Mach, F. J. Merceret, J. C. Willett and P. T. Willis, 2007: Electric fields, cloud microphysics and reflectivity in anvils of Florida thunderstorms, *J. Geophys. Res*, **112**, D11215, doi: 10.1029/2006JD007550.

——, J. E. and J.C. Willett, 2007: Observed enhancement of reflectivity and the electric field in long-lived Florida anvils, *Mon. Wea. Rev.,* **135**, 10, 3362-3380.

Garner, T., R. Lafosse, D. G. Bellue, and E. Priselac, 1997: Problems associated with identifying, observing, and forecasting detached thunderstorm anvils for space shuttle operations. 7th *Conf. on Aviation, Range, and Aerospace Meteorology*, *Amer. Meteor. Soc.*, Long Beach, CA.

Hagemeyer, B. C., and G. K. Schmocker, 1991: Characteristics of east-central Florida tornado environments. *Wea. Forecasting,* **6,** 499–514.

Krehbiel, P. R., 1986: The electrical structure of thunderstorms. In The Earth's Electrical Environment, National Academies Press, Washington, D.C., pp. 90–113.

——, P., W. Rison, R. Thomas, and H. Edens, 2009: Storm electrical structures and characteristics as indicated by VHF total lightning measurements. *Southern Thunder Workshop*, Cocoa Beach, FL.

Kuhlman, K. M., D. R. MacGorman, M. I. Biggerstaff, and P. R. Krehbiel, 2009: Lightning initiation in the anvils of two supercell storms. *Geophys. Res. Lett.*, **7**. doi: 10.1029/2008GL036650.

Lakshmanan, V., T. Smith, K. Hondl, G. J. Stumpf, and A. Witt, 2006: A real-time, three dimensional, rapidly updating, heterogeneous radar merger technique for reflectivity, velocity, and derived products. *Wea. Forecasting*, **21**, 802–823.

——, V., T. Smith, G. Stumpf, and K. Hondl, 2007: The Warning Decision Support System Integrated Information. *Wea. Forecasting*, **22**, 596–612.

Maier, L. M., C. Lennon, T. Britt, and S. Schaefer, 1995; Lightning Detection and Ranging (LDAR) system performance analysis, *6th Conf. on Aviation Weather Systems, Amer. Meteor. Soc.*, Dallas, TX.

McNamara, T. M., 2009: Four dimensional lightning surveillance system's (4DLSS) application in space launch weather support. *Southern Thunder Workshop*, Cocoa Beach, FL.

——, W. P. Roeder, and F. J. Merceret, 2010: The 2009 update to the lightning launch commit criteria. *14th Conf. ARAM, Amer. Meteor. Soc.*, Atlanta, GA.

Melvin, H. A., and H. E. Fuelberg, 2009: Developing a Nowcasting Scheme for Lightning Cessation at the Kennedy Space Center. *Southern Thunder Workshop*, Cocoa Beach, FL.

Merceret, F. J., J. G. Ward, D. M. Mach, M. G. Bateman, and J. E. Dye, 2008: On the magnitude of the electric field near thunderstorm-associated clouds, *J. Appl. Meteor. Clim.*, **47**, 240– 248.

——, F.J. and J.C. Willet, Editors, H.J. Christian, J.E. Dye, E.P. Krider, J.T. Madura, T.P. O'Brien, W.D. Rust, and R.L. Waltersheid, 2010: A History of the Lightning Launch Commit Criteria and the Lightning Advisory Panel for America's Space Program, *Lightning Advisory Panel*, NASA/SP-2010-216283, 2-6, 21, 251 pp.

Murphy, M. J., K. L. Cummins, and L. M. Maier, 2000: The analysis and interpretation of

three-dimensional lightning flash information, *16th International Conf. on IIPS for Meteorology, Oceanography, and Hydrology*, *Amer. Meteor. Soc.*, Long Beach, CA.

Patrick, G., 2009: Assessing lightning threat using Vaisala VHF total lightning mapping network data. *Southern Thunder Workshop*, Cocoa Beach, FL.

Roeder, and C. S. Pinder, 1998: Lightning Forecasting Empirical Techniques for Central Florida in Support of America's Space Program, *16th Conference on Weather Analysis and Forecasting*, 475-477.

——, W. P., J. T. Madura, and D. E. Harms, 2000: Lightning safety for personnel at Cape Canaveral Air Force Station and Kennedy Space Center, JANNAF/S&EPS, *CPIA Publ.* **698**, 59–70, Chem. Propul. Info. Agency, Columbia, MD.

——, and T. M. McNamara, 2006: A survey of the Lightning Launch Commit Criteria, *Second Conf. Meteor. App. Lightning Data*, *Amer. Meteor. Soc.*, Atlanta, GA.

——, W. P., 2010: The Four Dimension Lightning Surveillance System, *21st International Lightning Detection Conference*, 19-20, 15 pp.

Rudlosky S. D., and H. E. Fuelberg, 2010: Pre- and postupgrade distributions of NLDN reported cloud-to-ground lightning characteristics in the contiguous United States. *Mon. Wea. Rev.*, doi:10.1175/2010MWR3283.1.

Short, D. A., J. E. Sardonia, W. C. Lambert, and M. M. Wheeler, 2004: Nowcasting thunderstorm anvil clouds over Kennedy Space Center and Cape Canaveral Air Force Station. *Wea. Forecasting,* **19**, 706–713.

Stano, G. T., H. E. Fuelberg, and W. P. Roeder, 2010: Developing empirical lightning cessation forecast guidance for the Kennedy Space Center. *J. Geophys. Res.*, **115**, D09205, doi:10.1029/2009JD13034.

Ward, J. G., K. L. Cummins, E. P. Krider, 2008: Comparison of the KSC-ER Cloud-to-Ground Lightning Surveillance System (CGLSS) and the U.S. National Lightning Detection Network (NLDN), *20th International Lightning Detection Conf.*, Tucson, AZ.

Weems, J. W., C. S. Pinder, W. P. Roeder, B. F. Boyd, 2001: Lightning Watch and Warning Support to Spacelift Operations, *18th Conference on Weather Analysis and Forecasting*, 30 July-2 August 1, 301-305.

Weiss, S. A., D. M. MacGorman, and K. M. Kuhlman, 2009: Lightning in the anvils of supercells. *Southern Thunder Workshop*, Cocoa Beach, FL.

Willett, John C. and Francis J. Merceret, Editors, E. Philip Krider, James E. Dye, T. Paul O'Brien, W. David Rust, Richard L. Walterscheid, John T. Madura, and Hugh J. Christian, 2010: Rationales for the Lightning Flight Commit Criteria, NASA/TP-2010-216291, 1-2, 33-34, 251 pp.

Wilks, D.S., 2006, Statistical Methods in the Atmospheric Sciences (Second Edition), San Diego: Academic Press.